Efficiency and phase of optical parametric amplification in chirped quasi-phase-matched gratings

C. R. Phillips* and M. M. Fejer

E. L. Ginzton Laboratory, Stanford University, 450 Via Palou, Stanford, California 94305, USA
**Corresponding author: chris.phillips@stanford.edu*

Received June 8, 2010; revised August 8, 2010; accepted August 9, 2010;
posted August 24, 2010 (Doc. ID 129761); published September 9, 2010

Three-wave nonlinear interactions in chirped quasi-phase-matched (QPM) gratings are shown to exhibit conversion efficiency approaching 100% with increasing input pump and signal intensities, evading backconversion, as long as the idler vanishes at the input and the QPM grating is sufficiently chirped. The signal phase is described in terms of Kerr-like self- and cross-phase modulations, in the cascade $\chi^{(3)}$ approximation. Achieving high gain and efficiency simultaneously can lead to a large nonlinear phase, and the resulting trade-off is discussed.

OCIS codes: 140.4480, 190.4970, 190.4410, 190.7110.

Chirped quasi-phase-matched (QPM) gratings have been investigated for broadband and engineered frequency conversion in a variety of three-wave mixing configurations [1–4]. The grating k vector is varied smoothly over the length of the device, avoiding the bandwidth constraints associated with dispersion in the k vector mismatch: each spectral component is generated only around its phase-matched region in the grating, over a distance related to the local chirp rate.

The nonlinear coefficient of the chirped QPM grating $d(z)$ is defined as a function of position as segments of $+d_0$ and $-d_0$, where d_0 is the relevant projection on the nonlinear tensor. In the undepleted-pump and low-signal-gain limits there is a transfer function from the input waves to the generated idler wave, determined by the spatial Fourier transform of $d(z)$, with the mapping of spatial frequency (phase mismatch) to optical frequency of the transfer function determined by the dispersion of the nonlinear crystal [2]. The output of chirped QPM gratings can thus be engineered in both amplitude and phase. The phase-matched position is mapped to group delay of the generated wave by the group-velocity mismatch, and the amplitude spectrum is determined by the local chirp rate. These approaches were shown experimentally in [1,4] and theoretically in [5,6].

Interactions in chirped QPM gratings have also been shown to exhibit minimal backconversion [3], in contrast to phase-matched media or periodic QPM gratings. In the cases of sum frequency generation (SFG) and difference frequency generation (DFG), the interaction between idler and pump (assuming a strong and unamplified signal wave) corresponds to adiabatic following; provided that the grating is long enough and the signal is sufficiently intense, the three waves closely follow a local plane-wave eigenmode [3,7,8], which evolves smoothly with the QPM chirp.

Up until now, the nonlinear nature of the $\chi^{(2)}$ coupled wave equations has received less attention when analyzing chirped QPM gratings, with the interaction being linearized by the assumption that at least one of the three waves remains unchanged during propagation. This linearization is inappropriate for optical parametric amplification (OPA) schemes for which a key consideration is depletion of the pump. In this Letter, we investigate the behavior of chirped QPM interactions for which the amplitudes of all three waves change significantly during propagation. We find that useful properties from the linear regime can nonetheless be maintained, with conversion efficiency of the pump monotonically approaching 100% with increasing pump intensity for processes phase matched across the grating Fourier spectrum, even for high-gain OPA. We discuss the factors affecting the conversion efficiency in chirped QPM gratings, as well as the nonlinear phase accumulation, which places constraints on the maximum pump intensity.

Plane, cw interactions are assumed, relevant to the amplification of individual spectral components in a wide-beam, highly chirped-pulse OPA. We choose a normalization for the coupled envelope equations [6] based on the conserved sum of signal and pump photon fluxes. Assuming first-order QPM,

$$\begin{aligned} \dot{a}_i - i\delta k(\zeta) a_i &= -ig(\zeta) a_s^* a_p, \\ \dot{a}_s - i\delta k(\zeta) a_s &= -ig(\zeta) a_i^* a_p, \\ \dot{a}_p - i\delta k(\zeta) a_p &= -ig(\zeta) a_i a_s, \end{aligned} \tag{1}$$

where subscripts i, s, and p indicate quantities associated with idler, signal, and pump pulses, respectively. The field coupling coefficient is $\kappa = (\frac{\omega_i \omega_s \omega_p}{n_i n_s n_p})^{1/2} \frac{2}{\pi} \frac{d_0}{c}$, and the corresponding input signal and pump coupling coefficients are $\gamma_j = \kappa (\frac{n_j}{\omega_j})^{1/2} |E_j(z=0)|$ for $j = s$ and $j = p$, respectively, where E_j denotes the electric field for wave j. We assume that there is no input idler and normalize according to the total number of input photons using $\gamma_{sp} = (\gamma_s^2 + \gamma_p^2)^{1/2}$. Minor changes to these definitions could be performed for the case of no input pump (i.e., DFG). The normalized phase mismatch is $\delta k(z) = \Delta k(z)/\gamma_{sp}$, with $\Delta k(z) = k_p - k_s - k_i - K_g(z)$ for idler, signal, and pump carrier wave vectors k_i, k_s, and k_p, respectively. The normalized propagation coordinate is $\zeta = \gamma_{sp} z$, and overdots indicate derivatives with respect to ζ. The normalized fields are given by $a_j = \exp(i\phi_G) \frac{\kappa}{\gamma_{sp}} (\frac{n_j}{\omega_j})^{1/2} E_j$, where the accumulated grating phase $\phi_G(z) = \int_0^z \Delta k(z') \mathrm{d}z'$. The smooth grating phase $\phi_G(z)$ can be so defined when the QPM grating is written

$d(z)/d_0 = \mathrm{sgn}(\cos(\phi_G(z)))$. The function $0 \le g(\zeta) \le 1$ is a real-valued scaling of the nonlinear coefficient used for apodization of the QPM grating [6,9]. The ratio of signal and pump input photon fluxes is defined as $\rho = |a_s(0)/a_p(0)|^2$ and the pump depletion at $z = L$ as $\eta = |a_p(L)/a_p(0)|^2$, where L is the length of the grating; the conversion efficiency is then $(1 - \eta)$.

For chirped QPM gratings, the interaction between the waves is most simply illustrated by choosing a linear chirp profile, so $K_g(z) = K_{g0} - \kappa' z$, where κ' is the chirp rate ($\kappa' = -dK_g/dz = d\Delta k/dz$) and K_{g0} is a constant. For OPA in the undepleted-pump limit, the power gain for the signal is $G \approx \exp(2\pi\lambda_{R,p})$ where $\lambda_{R,p} \equiv \gamma_p^2/|\kappa'|$ [6]. For SFG in the unamplified-signal limit $\eta \approx \exp(-2\pi\lambda_{R,s})$ [3], where $\lambda_{R,s} \equiv \gamma_s^2/|\kappa'|$. These results apply for sufficiently chirped QPM gratings [3,6].

To understand the nonlinear regime, we plot in Fig. 1 the photon flux of the pump as a function of position with $\lambda_{R,p} = 2$ for several input-signal–photon-flux ratios parametrized by ρ. The first and last 7.5% of the grating is used for apodization [6] such that $|g/\delta k| \ll 1$ at $z = 0$ and $z = L$. The interaction is phase matched at $z = z_{\mathrm{pm}}$ and, in the absence of any pump depletion, amplification, would occur over the region $-1 < (z - z_{\mathrm{pm}})/L_{\mathrm{deph}} < 1$, where the dephasing length $L_{\mathrm{deph}} \equiv 2\gamma_p/|\kappa'|$ [6]. The pump is converted to the signal and idler within this amplification region with conversion efficiency that increases monotonically with signal intensity. Outside the amplification region, the fields exhibit oscillatory behavior, with low net energy transfer.

Numerical solutions of Eqs. (1) show that the conversion efficiency approaches 100% with large signal and pump intensities, and, hence, backconversion to the pump is suppressed at $z = L$. This behavior can be understood (for arbitrary ρ) through the adiabatic following of local nonlinear eigenmodes, in analogy to the following of linear eigenmodes in the SFG case ($\rho \gg 1$) [3,7,10,11]. The eigenmodes are those solutions of Eqs. (1) in the case of constant δk for which propagation corresponds only to phase shifts of the three waves, with $|a_j|$ constant. Up to an overall phase, there are two nontrivial eigenmodes for a given δk and set of input conditions. If $|\delta k(0)| \gg 1$ in a chirped grating, the input fields (with $a_i(0) = 0$) are close to one of these eigenmodes. As δk is varied, this eigenmode is swept from one corresponding to no photons at the idler frequency (input, with $\pm\delta k(0) \gg 1$) to one with no photons at the pump frequency (output, with $\mp\delta k(L) \gg 1$); the fields follow this eigenmode provided the chirp rate is slow. This adiabatic following process can be analyzed using the geometrical construction of [8], with motion of reduced field variables confined to a sphere for $\rho \gg 1$ [3,7] being replaced, for arbitrary ρ, by motion confined to the convex surface of [8]. This approach will be discussed in detail elsewhere.

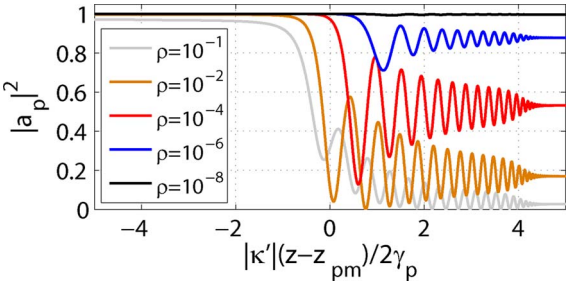

Fig. 1. (Color online) Pump depletion in an apodized QPM grating, with undepleted-pump gain set by $\lambda_{R,p} = 2$ and phase-matched point $z_{\mathrm{pm}} = L/2$, at increasing signal–pump-photon-flux ratio ρ.

To determine the effects of pump and signal intensity on conversion efficiency, we solve Eqs. (1) numerically. Figure 2 shows contours of η as a function of normalized parameters $\lambda_{R,p}$ and ρ for chirp length $\zeta_L \equiv \sqrt{\kappa' L} = 45$. For high signal gain and low conversion efficiency, $1 - \eta \approx \rho \exp(2\pi\lambda_{R,p}) \ll 1$, and, hence, contours of constant η are approximately straight lines in $[\log(\rho) - \lambda_{R,p}]$ space. The straight contours of Fig. 2, even when most of the pump is depleted, indicate that this scaling persists into the nonlinear regime. Similar plots for other ζ_L show that η, for wavelengths within the phase-matching bandwidth, is almost independent of ζ_L when $L \gg L_{\mathrm{deph}}$ and a suitable apodization profile is applied.

Given an upper limit on $\lambda_{R,p}$, Fig. 2 shows that high conversion efficiency (small η) cannot be achieved unless ρ is sufficiently large. To achieve high conversion efficiency for a fixed and small ρ, multiple amplification stages are then required such that ρ is large enough in the final power amplifier. In experiments, one will usually be limited to the moderate range of $\lambda_{R,p}$ considered in Fig. 2 due to a variety of considerations, including the damage threshold of the medium and the accumulation of nonlinear phase, which is considered below.

The contours of η as a function of $\log(\rho)$ and $\lambda_{R,p}$ are not straight for η small enough that $\ln(\eta) \ll -\pi$; they then depend on the separation of length scales required to support adiabaticity (rapid oscillations around slowly varying local eigenmodes). We do not illustrate this regime here, since such conversion efficiencies cannot be reached for $\rho < 10^{-1}$ given the practical range of $\lambda_{R,p}$ values under consideration.

We consider next the accumulation of signal phase in the QPM grating. This phase, which depends primarily on $\lambda_{R,p}$ and η, has application-dependent constraints associated with, for example, the requirements to avoid nonlinear focusing and to produce compressible amplified chirped pulses; both of these requirements place a limit on the nonlinear phase accumulated by the signal. The phase shifts accumulated can be understood, for $|\delta k| > 1$, by a multiple scale analysis of Eqs. (1) [12]. With $g = 1$, the analysis yields the following set of coupled

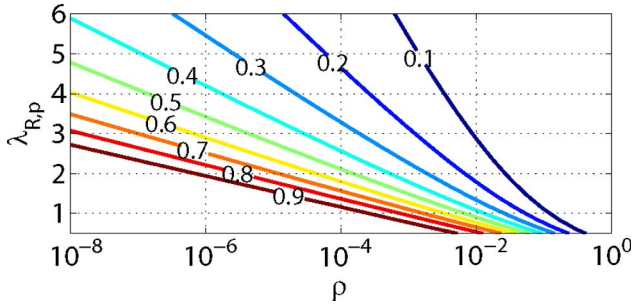

Fig. 2. (Color online) Transmitted pump η as a function of $\lambda_{R,p}$ and ρ, with $z_{\mathrm{pm}} = L/2$ and using $\sqrt{|\kappa'|}L = 45$ so that $L \gg 2L_{\mathrm{deph}}$ for all values of $\lambda_{R,p}$ simulated. Contours are labeled with values of η.

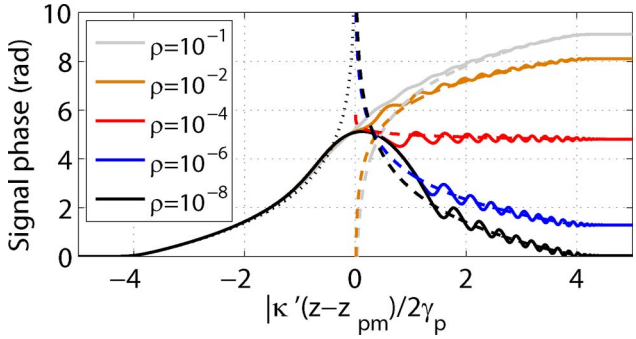

Fig. 3. (Color online) Signal phase accumulation during propagation with $\lambda_{R,p} = 2$ and $z_{\mathrm{pm}} = L/2$ at increasing signal-to-pump-photon-flux ratio ρ, obtained with numerical solution of Eqs. (1). The dotted and dashed curves are approximations to the phase, based on Eqs. (2), with $a_j^{(0)}(0) = a_j(0)$ and $a_j^{(0)}(\zeta_L) = a_j(\zeta_L)$.

effective nonlinear Schrödinger equations for leading order fields $a_j^{(0)}$, which vary slowly compared to $1/\delta k$ (except for the $\exp(-i\phi_G)$ envelope):

$$\begin{aligned}
\dot{a}_i^{(0)} - i\delta k(\zeta) a_i^{(0)} &= -i\delta k(\zeta)^{-1}[|a_p^{(0)}|^2 - |a_s^{(0)}|^2] a_i^{(0)},\\
\dot{a}_s^{(0)} - i\delta k(\zeta) a_s^{(0)} &= -i\delta k(\zeta)^{-1}[|a_p^{(0)}|^2 - |a_i^{(0)}|^2] a_s^{(0)},\\
\dot{a}_p^{(0)} - i\delta k(\zeta) a_p^{(0)} &= -i\delta k(\zeta)^{-1}[|a_i^{(0)}|^2 + |a_s^{(0)}|^2] a_p^{(0)}. \qquad (2)
\end{aligned}$$

From Eqs. (2), the rate of phase accumulation depends on both δk and the relative number of photons in the three waves. There is a sign change for the rate of signal phase accumulation from δk on passing through the phase-matched point z_{pm} [since $\delta k(z_{\mathrm{pm}}) = 0$] and also from $|a_p|^2 - |a_i|^2$ at the point where the pump becomes more than 50% depleted. We illustrate this behavior in Fig. 3, which plots numerical solutions of Eqs. (1) with $z_{\mathrm{pm}} = L/2$. The approximate phases calculated using Eqs. (2) agree with numerical solutions outside the amplification region, so they can be used to estimate the phases accumulated once η is known.

Further simulations show that the phase is approximately proportional to $\lambda_{R,p}$ at fixed η and ζ_L, and that the bandwidth of the device depends primarily on ζ_L, as in the linear case [6]. From Fig. 2, $\eta = 0.1$ at $\rho = 10^{-1}$ and $\lambda_{R,p} \approx 1$. From Fig. 3, an estimate for the phase with these parameters and $\zeta_L = 45$ is 1.5π rad. However, for $\eta = 0.1$ and $\rho = 10^{-3}$, $\lambda_{R,p} \approx 6$ is required, yielding a phase of more than 7π rad, exceeding the likely phase tolerances. Multiple amplification stages would be required in such a case. A lower value of ζ_L would reduce the phase, but also the amplification bandwidth, so this is another aspect of the trade-off.

In conclusion, we have considered the general three-wave nonlinear interaction in chirped QPM gratings. The remarkable efficiency and bandwidth properties seen previously in the undepleted-pump SFG regime are shown to be preserved in the nonlinear regime, with conversion efficiency approaching 100% with increasing input pump and signal intensities. Achieving high gain and efficiency simultaneously in a single chirped QPM grating may not be practical, in particular due to restrictions on the accumulated phase. These phases can be understood in terms of Kerr-like approximations, with the rate of phase accumulation changing sign when one of the input waves is depleted.

The understanding of nonlinear interactions in chirped QPM gratings developed here should help enable the design of high-gain, high-efficiency, and broad-bandwidth amplifier systems with engineered phase response, representing a promising approach to optical frequency conversion.

This research was supported by the U.S. Air Force Office of Scientific Research (USAFOSR) under grants FA9550-09-1-0233 and FA9550-05-1-0180.

References

1. M. Charbonneau-Lefort, B. Afeyan, and M. M. Fejer, J. Opt. Soc. Am. B **25**, 1402 (2008).
2. G. Imeshev, M. M. Fejer, A. Galvanauskas, and D. Harter, J. Opt. Soc. Am. B **18**, 534 (2001).
3. H. Suchowski, V. Prabhudesai, D. Oron, A. Arie, and Y. Silberberg, Opt. Express **17**, 12731 (2009).
4. L. Gallmann, G. Steinmeyer, U. Keller, G. Imeshev, M. M. Fejer, and J. Meyn, Opt. Lett. **26**, 614 (2001).
5. M. Charbonneau-Lefort, M. M. Fejer, and B. Afeyan, Opt. Lett. **30**, 634 (2005).
6. M. Charbonneau-Lefort, B. Afeyan, and M. M. Fejer, J. Opt. Soc. Am. B **25**, 463 (2008).
7. M. D. Crisp, Phys. Rev. A **8**, 2128 (1973).
8. G. Luther, M. Alber, J. Marsden, and J. Robbins, J. Opt. Soc. Am. B **17**, 932 (2000).
9. J. Huang, X. Xie, C. Langrock, R. Roussev, D. Hum, and M. M. Fejer, Opt. Lett. **31**, 604 (2006).
10. N. V. Vitanov, T. Halfmann, B. W. Shore, and K. Bergmann, Annu. Rev. Phys. Chem. **52**, 763 (2001).
11. N. V. Vitanov, Phys. Rev. A **59**, 988 (1999).
12. C. Conti, S. Trillo, P. Di Trapani, J. Kilius, A. Bramati, S. Minardi, W. Chinaglia, and G. Valiulis, J. Opt. Soc. Am. B **19**, 852 (2002).